$B \to (J/\psi, \eta_c)K$ decays in the perturbative QCD approach*

LIU Xin(刘新)[1)] ZHANG Zhi-Qing(张志清) XIAO Zhen-Jun(肖振军)[2)]

Department of Physics and Institute of Theoretical Physics, Nanjing Normal University, Nanjing 210046, China

Abstract In this paper, we calculated the $B \to (J/\psi, \eta_c)K$ decays in the perturbative QCD (pQCD) factorization approach with the inclusion of the partial next-to-leading order (NLO) contributions. With the inclusion of the significant enhancement from the NLO vertex corrections, the NLO pQCD predictions for the branching ratios agree with the data within 2σ errors: $Br(B^0 \to J/\psi K^0) = 5.2^{+3.5}_{-2.8} \times 10^{-4}$, $Br(B^+ \to J/\psi K^+) = 5.6^{+3.7}_{-2.9} \times 10^{-4}$, $Br(B^0 \to \eta_c K^0) = 5.5^{+2.3}_{-2.0} \times 10^{-4}$, $Br(B^+ \to \eta_c K^+) = 5.9^{+2.5}_{-2.1} \times 10^{-4}$.

Key words B meson, next-to-leading order corrections, branching ratio, perturbative QCD approach

PACS 13.25.Hw, 12.38.Bx, 14.40.Nd

1 Introduction

The $B \to J/\psi K$ and $B \to \eta_c K$ decays are phenomenologically very interesting decay modes and have drawn great attention for many years. Although the underlaying weak decay of $b \to c\bar{c}s$ is simple, a clear understanding of the exclusive $B \to (J/\psi, \eta_c)K$ decays is really difficult because it involves complex strong-interaction effects.

On the experimental side, the experimental measurements for $B \to J/\psi K_{S,L}$ decays result in the precision determination of $\sin 2\beta$ [1]. The branching ratios of $B \to (J/\psi, \eta_c)K$ decays have been measured with good or high precision [1, 2]. On the theoretical side, these decays have been studied intensively by employing various theoretical methods or approaches, for example, in Refs. [3–13]. Unfortunately, it is still very difficult to give satisfactory explanation for the corresponding data without worrying about the serious problems.

For $B \to J/\psi K$ decay, for example, the theoretical predictions for its branching ratio in both the naive factorization approach [4] and the QCD factorization (QCDF) approach [14] are much smaller (a factor of 7–10) than the measured values [5]. In Refs. [8, 9], the QCDF prediction is $Br(B \to \eta_c K) = 1.9 \times 10^{-4}$, a factor of 5 smaller than the measured value, after the inclusion of the twist-3 part of kaon. The predictions obtained by employing the QCD light-cone sum rules [10] are also too small to accommodate the data.

In Refs. [12, 13], the authors employed the QCDF approach to calculate the factorizable contributions, but the pQCD approach [11] to evaluate the non-factorizable part to the considered decays. In this way, they found a large $Br(B \to J/\psi K)$ comparable with the data, but a small (a factor of 3) $Br(B \to \eta_c K)$. Furthermore, it should be mentioned that these results [12, 13] were obtained by treating one decay with two different factorization approaches: the self-consistency of such a "mixing-approach" may be a serious problem.

Up to now, there has been not a clear and satisfactory theoretical interpretation for the measured large decay rates of $B \to (J/\psi, \eta_c)K$. We call this situation the "$B \to (J/\psi, \eta_c)K$" puzzle. In this paper, we will calculate the branching ratios of the four $B \to (J/\psi, \eta_c)K$ decays by employing the pQCD factorization approach. Besides the full leading order (LO) contributions, the currently known next-to-leading order (NLO) contributions [15] will also be included.

Received 17 September 2009, Revised 24 November 2009

∗ Supported by National Natural Science Foundation of China (10605012, 10735080) and Project on Graduate Students' Education and Innovation of Jiangsu Province (CX09B_297Z)

1) E-mail: js.xin.liu@gmail.com

2) E-mail: xiaozhenjun@njnu.edu.cn

The paper is organized as follows: in Sec. 2, we first present the formalism of the pQCD approach, and then make the analytic calculations and show the decay amplitudes for the considered decays. In Sec. 3, we show the numerical results and compare them with the measured values. A short summary and some conclusions are also given in this section.

2 Formalism and perturbative calculations

2.1 Formalism

In recent years, the pQCD factorization approach has been used frequently to calculate various B meson decay channels. In Ref. [16], the $B\to J/\psi K$ decays have been studied by employing the pQCD approach at leading order. Here we try to apply the pQCD approach to calculate the $B\to(J/\psi,\eta_c)K$ decays with the inclusion of the partial NLO corrections.

Using the light-cone coordinates the B meson and the two final state meson momenta can be written as

$$\begin{aligned} P_1 &= \frac{m_B}{\sqrt{2}}(1,1,0_T), \quad P_2=\frac{m_B}{\sqrt{2}}(1,r^2,0_T),\\ P_3 &= \frac{m_B}{\sqrt{2}}(0,1-r^2,0_T), \end{aligned} \tag{1}$$

respectively, where $r=m_{M_2}/m_B$, and the light mass $m_{M_3}=m_K$ has been neglected. The longitudinal polarization of vector J/ψ, ϵ_L, is defined as

$$\epsilon_L=\frac{m_B}{\sqrt{2}m_{J/\psi}}(1,-r^2_{J/\psi},0_T).$$

Putting the light (anti-) quark momenta in B and M_3 mesons as k_1 and k_3, respectively, we can choose: $k_1=(x_1P_1^+,0,\boldsymbol{k}_{1T})$ and $k_3=(0,x_3P_3^-,\boldsymbol{k}_{3T})$. For $M_2=(J/\psi,\eta_c)$, the momentum fraction of c quark is chosen as x_2P_2. Then, by integration over k_1, k_2, and k_3, the decay amplitude of $B\to M_2M_3$ decays in the pQCD approach can be written conceptually as the convolution,

$$\begin{aligned} \mathcal{A}(B\to M_2M_3) \sim \int &dx_1dx_2dx_3b_1db_1b_2db_2b_3db_3\times\\ &\mathrm{Tr}\Big[C(t)\Phi_B(x_1,b_1)\Phi_{M_2}(x_2,b_2)\times\\ &\Phi_{M_3}(x_3,b_3)H(x_i,b_i,t)S_t(x_i)e^{-S(t)}\Big], \end{aligned} \tag{2}$$

where b_i is the conjugate space coordinate of k_{iT}, and t is the largest energy scale in function $H(x_i,b_i,t)$. The large logarithms $\ln(m_W/t)$ are included in the Wilson coefficients $C(t)$. The large double logarithms $(\ln^2 x_i)$ on the longitudinal direction are summed by the threshold resummation [17], and they lead to $S_t(x_i)$ which smears the end-point singularities on x_i. The last term, $e^{-S(t)}$, is the Sudakov form factor which suppresses the soft dynamics effectively [18].

For the considered decays, the weak effective Hamiltonian $\mathcal{H}_{eff}$ can be written as

$$\begin{aligned} \mathcal{H}_{eff} = \frac{G_F}{\sqrt{2}}\Big[&V_{cb}^*V_{cs}\left(C_1(\mu)O_1^c(\mu)+C_2(\mu)O_2^c(\mu)\right)-\\ &V_{tb}^*V_{ts}\sum_{i=3}^{10}C_i(\mu)\,O_i(\mu)\Big], \end{aligned} \tag{3}$$

where $C_i(\mu)$ are the Wilson coefficients at the renormalization scale μ and O_i are the four-fermion operators for the case of $\bar{b}\to\bar{s}$ transition

When the pQCD approach at LO (NLO) is employed, the LO (NLO) Wilson coefficients $C_i(m_W)$ and $\alpha_s(t)$ will be used. We take $\Lambda^{(5)}_{QCD}=0.225$ GeV, $\Lambda^{(4)}_{QCD}=0.287$ GeV (0.326 GeV) for LO (NLO) case. As discussed in Refs. [19, 20], it is reasonable to choose $\mu_0=1.0$ GeV as the lower cut-off of the hard scale t. In the numerical integrations we will fix the values $C_i(t)$ at $C_i(1.0)$ whenever the scale t runs below the scale $\mu_0=1.0$ GeV [19, 20], unless otherwise stated.

2.2 $B\to J/\psi M_3$ decays at leading order

At the leading order pQCD approach, the Feynman diagrams for the considered decays are shown in Fig. 1. After the analytical calculation, we found the the total decay amplitude for the decays $B\to J/\psi M_3$ ($M_3=K^\pm,K^0$):

$$\begin{aligned} \mathcal{M}(B\to J/\psi M_3) = F_{J/\psi M_3}f_{J/\psi}\Big\{&V_{cb}^*V_{cs}\,a_2-\\ &V_{tb}^*V_{ts}\left(a_3+a_5+a_7+a_9\right)\Big\}+\\ M_{J/\psi M_3}\Big\{&V_{cb}^*V_{cs}C_2-\\ &V_{tb}^*V_{ts}\left(C_4-C_6-C_8+C_{10}\right)\Big\}, \end{aligned} \tag{4}$$

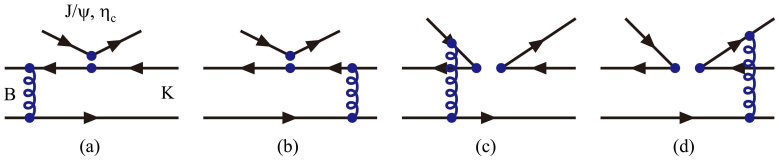

Fig. 1. Typical Feynman diagrams contributing to $B\to(J/\psi,\eta_c)K$ decays at leading order.

where $f_{J/\psi}$ is the decay constant of J/ψ meson, a_i is the combination of the Wilson coefficients C_i [19], while the factorizable and non-factorizable parts are of the form

$$\begin{aligned}F_{J/\psi M_3} &= 8\pi C_F m_B^2\int_0^1 dx_1 dx_3\int_0^\infty b_1 db_1 b_3 db_3\,\phi_B(x_1,b_1)\times\\ &\Big\{\Big[[(1-r^2)(1+x_3)-x_3r^2]\,\phi_{M_3}^A(x_3)+r_0(1-2x_3)\left[\phi_{M_3}^P(x_3)+\phi_{M_3}^T(x_3)\right]-\\ &r_0r^2\left[(1-2x_3)\phi_{M_3}^P(x_3)-(1+2x_3)\phi_{M_3}^T(x_3)\right]\Big]\alpha_s(t_e^1)\,h_e(x_1,x_3,b_1,b_3)\exp\left[-S_{ab}(t_e^1)\right]+\\ &2r_0\,(1-r^2)\,\phi_{M_3}^P(x_3)\cdot\alpha_s(t_e^2)h_e(x_3,x_1,b_3,b_1)\exp\left[-S_{ab}(t_e^2)\right]\Big\},\end{aligned}\tag{5}$$

$$\begin{aligned}M_{J/\psi M_3} &= -\frac{16\sqrt{6}}{3}\pi C_F m_B^2\int_0^1 dx_1 dx_2\,dx_3\int_0^\infty b_1 db_1 b_2 db_2\,\phi_B(x_1,b_1)\times\\ &\Big\{2rr_c\phi_{J/\psi}^t(x_2)\phi_{M_3}^A(x_3)-4rr_0r_c\phi_{J/\psi}^t(x_2)\,\phi_{M_3}^T(x_3)-[x_3+2(x_2-x_3)r^2]\,\phi_{J/\psi}^L(x_2)\phi_{M_3}^A(x_3)+\\ &2r_0\left[x_3+(2x_2-x_3)r^2\right]\phi_{J/\psi}^L(x_2)\phi_{M_3}^T(x_3)\Big\}\alpha_s(t_f)h_f(x_1,x_2,x_3,b_1,b_2)\exp\left[-S_{cd}(t_f)\right],\end{aligned}\tag{6}$$

where $r_0=m_0^K/m_B$, $r_c=m_c/m_B$, and $C_F=4/3$ is a color factor. The hard function h_e and the Sudakov factors S_{ab} are similar to those as given in Ref. [19]. The scales t_e^i and t_f are of the form

$$\begin{aligned}t_e^1 &= \max(\sqrt{x_3(1-r^2)}m_B,1/b_1,1/b_3),\\ t_e^2 &= \max(\sqrt{x_1(1-r^2)}m_B,1/b_1,1/b_3),\\ t_f &= \max(\sqrt{x_1x_3(1-r^2)}m_B,\\ &\quad\sqrt{(x_1-x_2)(x_3+(x_2-x_3)r^2+r_c^2)}m_B,\\ &\quad 1/b_1,1/b_2),\end{aligned}\tag{7}$$

where $r=m_{M_2}/m_B(M_2=J/\psi,\eta_c)$, $r_c=m_c/m_B$.

2.3 $B\to\eta_cM_3$ decays at leading order

Following the same procedure as for $B\to J/\psi K$ decays, it is straightforward to calculate the decay amplitudes for $B\to\eta_cM_3$ decays.

$$\begin{aligned}\mathcal{M}(B\to\eta_cM_3) &= F_{\eta_cM_3}f_{\eta_c}\left[V_{cb}^*V_{cs}\,a_2-\right.\\ &\left.V_{tb}^*V_{ts}\,(a_3+a_5+a_7+a_9)\right]+\\ &M_{\eta_cM_3}\left[V_{cb}^*V_{cs}C_2-V_{tb}^*V_{ts}\,(C_4+C_6+C_8+C_{10})\right],\end{aligned}\tag{8}$$

where the functions $F_{\eta_cM_3}, M_{\eta_cM_3}$, etc., are of the form

$$\begin{aligned}F_{\eta_cM_3} &= 8\pi C_F m_B^2\int_0^1 dx_1 dx_3\int_0^\infty b_1 db_1 b_3 db_3\,\phi_B(x_1,b_1)\times\\ &\Big\{\Big[[(1-r^2)(1+x_3)-x_3r^2]\,\phi_{M_3}^A(x_3)+r_0(1-2x_3)\left[\phi_{M_3}^P(x_3)+\phi_{M_3}^T(x_3)\right]+\\ &r_0r^2\left[(1+2x_3)\phi_{M_3}^P(x_3)-(1-2x_3)\phi_{M_3}^T(x_3)\right]\Big]\alpha_s(t_e^1)\,h_e(x_1,x_3,b_1,b_3)\exp[-S_{ab}(t_e^1)]+\\ &2r_0\,(1-r^2)\,\phi_{M_3}^P(x_3)\cdot\alpha_s(t_e^2)h_e(x_3,x_1,b_3,b_1)\exp[-S_{ab}(t_e^2)]\Big\},\end{aligned}\tag{9}$$

$$\begin{aligned}M_{\eta_cM_3} &= -\frac{16\sqrt{6}}{3}\pi C_F m_B^2\int_0^1 dx_1 dx_2 dx_3\int_0^\infty b_1 db_1 b_2 db_2\,\phi_B(x_1,b_1)\phi_{\eta_c}^v(x_2,b_2)\times\\ &x_3\Big[(1-2r^2)\,\phi_{M_3}^A(x_3)-2r_0\,(1-r^2)\,\phi_{M_3}^T(x_3)\Big]\alpha_s(t_f)h_f(x_1,x_2,x_3,b_1,b_2)\exp[-S_{cd}(t_f)],\end{aligned}\tag{10}$$

where $\phi_{\eta_c}^v$ is the leading twist-2 part of the distribution amplitude for the pseudo-scalar meson η_c.

2.4 NLO contributions in pQCD approach

In the pQCD approach, the NLO contributions may come from different sources [15, 19]. For the considered $B\to J/\psi K$ and η_cK decays, only the vertex corrections among the known NLO contributions [15, 19] will contribute.

For the four vertex correction diagrams [14, 15],

the infrared divergences from the soft gluons and collinear gluons in the four diagrams will be cancelled by each other, respectively. So the total contributions of these four figures are infrared finite. In other words, these vertex corrections can be calculated without considering the transverse momentum effects of the quark at the end-point region in collinear factorization theorem. Therefore, there is no need to employ the $k_{\rm T}$ factorization theorem here [15]. The vertex corrections to the $\rm B\to J/\psi K$ decays, denoted as $f_{\rm I}$ in QCDF, have been calculated in the NDR scheme [5, 6], and can be adopted directly. For $\rm B\to \eta_c K$ decays, the NLO vertex corrections can be included in the same way.

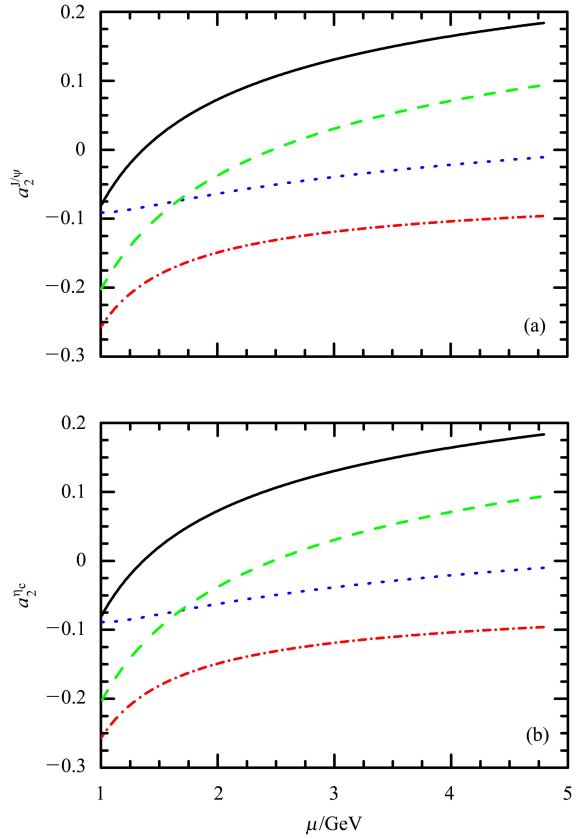

Fig. 2. Dependence of a_2 on the renormalization scale μ for (a) $\rm B\to J/\psi K$ and (b) $\rm B\to \eta_c K$ decays. The solid (dashed) curve stands for a_2 at NLO (LO) level without the vertex corrections, while the dotted (dash-dotted) curve refers to the real (imaginary) part of the a_2 at NLO level with the vertex corrections.

Since both $\rm B\to J/\psi K$ and $\rm \eta_c K$ are color-suppressed decays, the Wilson coefficient a_2 will play the dominant role:

$$a_2 = C_1+\frac{C_2}{3}+\frac{\alpha_{\rm s}}{4\pi}\frac{C_{\rm F}}{3}C_2\left(-18+12\ln\frac{m_{\rm b}}{\mu}+f_{\rm I}\right), \tag{11}$$

with the function $f_{\rm I}$

$$f_{\rm I} = \frac{2\sqrt{2N_{\rm c}}}{f_{\rm J/\psi}}\int {\rm d}x_2\phi^{\rm L}_{\rm J/\psi}(x_2)\left[\frac{3(1-2x_2)}{1-x_2}\ln x_2 - 3\pi{\rm i}+3\ln(1-r_2^2)+\frac{2r_2^2(1-x_2)}{1-r_2^2x_2}\right], \tag{12}$$

for $\rm B\to J/\psi K$ decays, where $r_2=m_{\rm J/\psi}/m_{\rm B}$.

For the $\rm B\to \eta_c K$ decays, we adopt the same function $f_{\rm I}$ as in Eq. (12), but by replacing $f_{\rm J/\psi}$ and $\phi^{\rm L}_{\rm J/\psi}$ with $f_{\rm \eta_c}$ and $\phi^{\rm v}_{\rm \eta_c}$, and setting $r_2=m_{\rm \eta_c}/m_{\rm B}$, respectively. Some arguments are as follows: In Ref. [9], the authors calculated the vertex corrections for $\rm B\to \eta_c K$ decays by taking the twist-3 distribution amplitude $\phi^{\rm s}_{\rm \eta_c}$ with the structure γ_5 as the leading twist one. But based on the discussion in Ref. [12], the infrared divergences in the vertex corrections to the $\rm B\to \eta_c K$ decays cancel only for the term proportional to $\gamma_5\not{P}$, i.e. the leading twist one. For the twist-3 part, the infrared divergence may still exist [12]. We here therefore use the leading twist distribution amplitudes only. At the leading order, the function $f_{\rm I}$ is process independent: the same form for both considered decays. Specifically, $\phi^{\rm L}_{\rm J/\psi}$ and $\phi^{\rm (v)}_{\rm \eta_c}$ are the same in form at leading order; while the difference between the decay constant $f_{\rm J/\psi}=0.405\pm0.014$ GeV and $f_{\rm \eta_c}=0.420\pm0.050$ GeV is indeed very small.

It is instructive to check the variation of a_2 with or without the inclusion of the NLO vertex corrections. From Figs. 2(a) and 2(b), one can see that (a) the μ-dependence of $a_2(\rm J/\psi K)$ and $a_2(\rm \eta_c K)$ is very similar, the small difference between the numerical values of a_2 are induced by using similar but different decay constants and r_2; (b) the μ-dependence of a_2 is decreased effectively due to the inclusion of the NLO vertex corrections; and (c) the vertex correction provides a large imaginary part to a_2, and therefore an effective enhancement of $|a_2|$ is expected.

3 Numerical results and discussions

The input parameters and the wave functions to be used in the numerical calculations are given in Appendix A.

Now we calculate the branching ratios for those considered decay modes. With the complete decay amplitudes, we can obtain the decay width for the considered decays,

$$\Gamma(\rm B\to M_2K)=\frac{G_{\rm F}^2m_{\rm B}^3}{32\pi}(1-r^2)\left|\mathcal{M}(\rm B\to M_2K)\right|^2, \tag{13}$$

where $r=m_{\rm J/\psi}/m_{\rm B}$ or $m_{\rm \eta_c}/m_{\rm B}$.

By using the input parameters and wave functions as given in Appendix A, we find the LO and NLO pQCD predictions (in unit of 10^{-4}) for the CP-averaged branching ratios of the four $B \to J/\psi K$ and $\eta_c K$ decays and show them in Table 1. The predictions listed in column one (two) are the LO (NLO) pQCD predictions. The first theoretical error in these entries arises from the B meson wave function shape parameter $\omega_b = 0.40 \pm 0.04$ and the decay constants $f_{J/\psi} = 0.405 \pm 0.014$ GeV and/or $f_{\eta_c} = 0.420 \pm 0.050$ GeV. The second error is from the combination of the uncertainties of Gegenbauer moments $a_1^K = 0.17 \pm 0.17$ and/or $a_2^K = 0.115 \pm 0.115$. In the fourth column of Table 1, as a comparison, we also cite the typical theoretical predictions obtained previously by using various approaches or models [5, 6, 9, 10]. In the last column of Table 1, we list the world averages of the experimental measurements [1, 2]. One can see that the LO pQCD predictions for the branching ratios are indeed much smaller than the measured values. When the NLO enhancement is included, however, the pQCD predictions are basically consistent with the data within the still large theoretical errors. Of course, the central values are still about 40% smaller than the measured values. There is still some room left for non-perturbative contributions.

The LO pQCD predictions for the branching ratios of $B \to J/\psi K$ decays in Table 1 are about half of those as given in Ref. [16]. The main reason is the introduction of a new lower cut-off of hard scale "t". In the current work, we set a lower cut-off for the hard scale "t", $t_{\min} = \mu_0 = 1.0$ GeV, in the numerical integrations. In previous work [16], however, the lower limit is $\mu_0 = 0.5$ GeV.

From general knowledge, the hard scale t must be much larger than $\Lambda_{QCD} \approx 0.2$ GeV in order to guarantee the reliability of perturbative calculations. It may be conceptually incorrect to evaluate the Wilson coefficients at scales as low as 0.5 GeV [21]. The explicit numerical evaluations of $C_i(\mu)$ in the range of $0.5 \leqslant \mu \leqslant 2.0$ GeV in Ref. [20] show that the μ-dependence of $C_i(\mu)$ becomes weak in the range of $\mu \geqslant 1.0$ GeV. We therefore believe that it is reasonable to choose $\mu_0 = 1.0$ GeV as the lower cut-off of the hard scale t, which is also close to the hard-collinear scale $\sqrt{\bar{\Lambda} m_B} \sim 1.3$ GeV in SCET.

Table 1. The LO and NLO pQCD predictions (in unit of 10^{-4}) of $Br(B \to J/\psi K)$ and $Br(B \to \eta_c K)$. For comparison, we also cite the typical theoretical predictions as given in previous literature (in the fourth column), and the measured values [1, 2].

channels	LO	NLO	others	data
$B^0 \to J/\psi K^0$	$1.1^{+0.8+0.9}_{-0.5-0.5}$	$5.2^{+1.0+3.4}_{-0.9-2.6}$	~ 1.0 [5]	8.71 ± 0.32
$B^+ \to J/\psi K^+$	$1.2^{+0.9+0.9}_{-0.5-0.5}$	$5.6^{+1.0+3.6}_{-0.9-2.8}$	~ 3.3 [10]	10.07 ± 0.35
$B^0 \to \eta_c K^0$	$0.8^{+0.5+0.1}_{-0.3-0.1}$	$5.5^{+2.1+1.0}_{-1.7-1.0}$	~ 2 [9, 12]	8.9 ± 1.6
$B^+ \to \eta_c K^+$	$0.8^{+0.5+0.2}_{-0.2-0.1}$	$5.9^{+2.2+1.2}_{-1.8-1.1}$	~ 2 [10, 12]	9.1 ± 1.3

Now we investigate in more detail why the vertex corrections can provide a significant enhancement. The total decay amplitudes as given in Eqs. (4) and (8) can be re-written as

$$M = [F_C + F_P]_{\text{Fac.}} + [M_T + M_P]_{\text{Spec.}}, \qquad (14)$$

where F_C and F_P stand for the "color-suppressed" and the penguin part of the factorizable contribution, coming from the emission diagram Fig. 1(a) and 1(b); while M_T and M_P stand for the "Tree" and the "Penguin" part of the nonfactorizable contribution, coming from the spectator diagram Fig. 1(c) and 1(d). From Eq. (4), for example, it is easy to separate the total decay amplitude $\mathcal{M}(B \to J/\psi K)$ into the following four parts

$$\begin{aligned} F_C &= F^{V-A}_{J/\psi K} f_{J/\psi} V^*_{cb} V_{cs}\, a_2; \\ F_P &= -F^{V-A}_{J/\psi K} f_{J/\psi} V^*_{tb} V_{ts}\, (a_3 + a_5 + a_7 + a_9); \qquad (15) \\ M_T &= M^{V-A}_{J/\psi K} V^*_{cb} V_{cs}\, C_2; \\ M_P &= -M^{V-A}_{J/\psi K} V^*_{tb} V_{ts}\, (C_4 - C_6 - C_8 + C_{10}). \qquad (16) \end{aligned}$$

By numerical calculations, we find easily the numerical values (in unit of 10^{-3}) of the individual parts and the total decay amplitude of $\mathcal{M}(B \to J/\psi K)$ at the LO and NLO level:

$$\begin{aligned} \mathcal{M}^{LO} = &\underbrace{-1.147}_{F_C} \underbrace{-0.092}_{F_P} + \underbrace{(1.487 + i0.529)}_{M_T} + \\ &\underbrace{(0.046 + i0.004)}_{M_P}, = 0.294 + i0.533, \qquad (17) \end{aligned}$$

$$\mathcal{M}^{\rm NLO} = \underbrace{(-0.546-{\rm i}1.433)}_{F_{\rm C}} + \underbrace{(0.004-{\rm i}0.038)}_{F_{\rm P}} + \underbrace{(1.367+{\rm i}0.485)}_{M_{\rm T}} + \underbrace{(0.037+{\rm i}0.002)}_{M_{\rm P}}, = 0.862-{\rm i}0.984, \quad (18)$$

and the ratio of the square of the decay amplitude $\mathcal{M}^{\rm NLO}$ and $\mathcal{M}^{\rm LO}$ is

$$R_{\rm M}({\rm B}\to {\rm J/\psi K}) = \frac{|\mathcal{M}^{\rm NLO}|^2}{|\mathcal{M}^{\rm LO}|^2} = 4.62. \quad (19)$$

For $\rm B \to \eta_c K$ decay, we find the similar result: $R_{\rm M}({\rm B}\to\eta_{\rm c}{\rm K}) = 7.0$.

From the above numerical results, it is easy to see that

(1) As generally expected, both $F_{\rm P}$ and $M_{\rm P}$ are always small in magnitude (less than 10%), when compared with $M_{\rm T}$ and $F_{\rm C}$.

(2) At LO, $F_{\rm C} = -1.147$ is large in size, but largely cancelled by the real part of $M_{\rm T}$ ($\mathrm{Re}(M_{\rm T}) = 1.487$) This strong cancellation results in a small LO pQCD prediction for the decay rates.

(3) At NLO, the real part of $F_{\rm C}$ changes from -1.147 to -0.546, the previous large cancellation between the real parts of $F_{\rm C}$ and $M_{\rm T}$ becomes significantly weak, while a large imaginary part $\mathrm{Im}(F_{\rm C}) = -1.433$ is also produced. These two changes lead to a large $|\mathcal{M}^{\rm NLO}|^2$ and consequently a large NLO pQCD prediction of the branching ratios.

(4) Although the NLO pQCD predictions for the branching ratios of the considered decays are consistent with the data within the still large theoretical uncertainties, the central values of the NLO pQCD predictions, as listed in Table 1, are still about 60% of the measured values. Certainly, there is still some room left for the non-perturbative long distance effects or other unknown higher order corrections.

(5) Among the three kinds of known NLO contributions in the pQCD approach, only the vertex corrections are relevant to $\rm B \to (J/\psi, \eta_c)K$ decays and taken into account here. Other possible NLO contributions coming from the Feynman diagrams as shown in Figs. 5–7 in Ref. [19] are still unknown at present but they are generally expected to be the small part of the NLO contributions in the pQCD factorization approach [15, 19].

In short, from the above pQCD predictions for the branching ratios and the detailed phenomenological analysis, we can conclude that the pQCD predictions for the branching ratios become close to the data due to the significant enhancement of the NLO vertex corrections.

In this paper, we calculated the branching ratios of the four $\rm B \to (J/\psi, \eta_c)K$ decays by employing the pQCD factorization approach. The inclusion of the NLO vertex contributions can provide a significant enhancement to the leading order pQCD predictions. Although the central values of the pQCD predictions are still 40% smaller than the measured ones, they basically agree with the data within 2σ errors.

Because only those currently known NLO contributions have been taken into account here, to obtain complete NLO calculations in the pQCD approach, the still missing pieces should be evaluated as soon as possible.

The authors are very grateful to Hsiang-nan Li, Cai-Dian Lü and Ying Li for valuable discussions.

Appendix A

Input parameters and wave functions

The masses, decay constants, QCD scale and B meson lifetime are the following

$$\begin{aligned} f_{\rm J/\psi} &= 0.405\ {\rm GeV}, \quad f_{\rm K} = 0.16\ {\rm GeV}, \quad f_{\eta_{\rm c}} = 0.42\ {\rm GeV}, \\ m_{\rm W} &= 80.41\ {\rm GeV}, \ m_{\eta_{\rm c}} = 2.98\ {\rm GeV}, \ m_{\rm B} = 5.2794\ {\rm GeV}, \\ m_{\rm J/\psi} &= 3.097\ {\rm GeV}, \quad \tau_{\rm B^+} = 1.643\ {\rm ps}, \quad \tau_{\rm B^0} = 1.53\ {\rm ps}. \end{aligned} \quad (A1)$$

For the CKM matrix elements, here we adopt the Wolfenstein parametrization for the CKM matrix, and take $\lambda = 0.2257, A = 0.814, \bar{\rho} = 0.135$ and $\bar{\eta} = 0.349$ [1].

As for the B meson wave function, we make use of the same parameterizations as in Ref. [22]. We adopt the model

$$\phi_{\rm B}(x,b) = N_{\rm B} x^2(1-x)^2 \exp\left[-\frac{m_{\rm B}^2\, x^2}{2\omega_{\rm b}^2} - \frac{1}{2}(\omega_{\rm b} b)^2\right], \quad (A2)$$

where $\omega_{\rm b}$ is a free parameter and we take $\omega_{\rm b} = 0.40 \pm 0.04$ GeV in numerical calculations, and $N_{\rm B} = 91.745$ is the normalization factor for $\omega_{\rm b} = 0.40$.

For the vector J/ψ and pseudoscalar $\eta_{\rm c}$ meson, we take the wave functions as follows,

$$\Phi_{\rm J/\psi}(x) = \frac{1}{\sqrt{2N_{\rm c}}}\Big\{ m_{\rm J/\psi} \not{\epsilon}_{\rm L} \phi_{\rm J/\psi}^{\rm L}(x) + \not{\epsilon}_{\rm L} \not{P} \phi_{\rm J/\psi}^{\rm t}(x) \Big\}, \quad (A3)$$

$$\Phi_{\eta_c}(x) = \frac{\mathrm{i}}{\sqrt{2N_c}}\gamma_5\left\{\not{P}\phi^{\mathrm{v}}_{\eta_c} + m_{\eta_c}\phi^{\mathrm{s}}_{\eta_c}\right\}, \qquad \text{(A4)}$$

respectively, where x represents the momentum fraction of the charm quark inside the charmonium. The twist-2 and twist-3 asymptotic distribution amplitudes, ϕ^{L}, ϕ^{v} and ϕ^{t}, ϕ^{s}, can be found in Ref. [23] and the twist-2 kaon distribution amplitude $\phi^{\mathrm{A}}_{\mathrm{K}}$, and the twist-3 ones $\phi^{\mathrm{P}}_{\mathrm{K}}$ and $\phi^{\mathrm{T}}_{\mathrm{K}}$ have been parameterized as given in Ref. [24].

References

1 Particle Data Group. Phys. Lett. B, 2008, **667**: 1
2 Heavy Flavor Averaging Group, Barberio E et al. arXiv: 0808.1297[hep-ex]; and online update at http://www.slac.stanford.edu/xorg/hfag
3 Gourdin M, Keum Y Y, Pham X Y. Phys. Rev. D, 1995, **51**: 3510
4 CHENG H Y, YANG K C. Phys. Rev. D, 1999, **59**: 092004
5 Chay J, Kim C. arXiv:0009244[hep-ph]
6 CHENG H Y, YANG K C. Phys. Rev. D, 2001, **63**: 074011
7 Boos H, Reuter J, Mannel T. Phys. Rev. D, 2004, **70**: 036006; Ciuchini M, Pierini M, Silvestrini L. Phys. Rev. Lett., 2005, **95**: 221804
8 SONG Z Z, MENG C, GAO Y J, CHAO K T. Phys. Rev. D, 2004, **69**: 054009; SONG Z Z, CHAO K T. Phys. Lett. B, 2003, **568**:127
9 SONG Z Z, MENG C, CHAO K T. Eur. Phys. J. C, 2004, **36**: 365; MENG C, GAO Y J, CHAO K T. Commun. Theor. Phys., 2007, **48**: 885
10 Melić B. Phys. Rev. D, 2003, **68**: 034004; Phys. Lett. B, 2004, **591**: 91; LI L, WANG Z G, HUANG T. Phys. Rev. D, 2004, **70**: 074006
11 CHANG C H V, LI H N. Phys. Rev. D, 1997, **55**: 5577; Yeh T W, LI H N. Phys. Rev. D, 1997, **56**: 1615
12 CHEN C H, LI H N. Phys. Rev. D, 2005, **71**: 114008
13 LI H N, Mishima S. J. High Energy Phys., 2007, **03**: 009
14 Beneke M, Buchalla G, Neubert N, Sachrajda C T. Phys. Rev. Lett., 1999, **83**: 1914
15 LI H N, Mishima S, Sanda A I. Phys. Rev. D, 2005, **72**: 114005
16 XIAO Z J, LIU X. Int. J. Mod. Phys. A, 2008, **23**: 3246
17 LI H N. Phys. Rev. D, 2002, **66**: 094010
18 LI H N, Tseng B. Phys. Rev. D, 1998, **57**: 443
19 XIAO Z J, ZHANG Z Q, LIU X, GUO L B. Phys. Rev. D, 2008, **78**: 114001
20 ZHANG Z Q, XIAO Z J. Eur. Phys. J. C, 2009, **59**: 49
21 Beneke M. Nucl. Phys. B(Proc.Suppl.), 2007, **170**: 57
22 LÜ C D, Ukai K, YANG M Z. Phys. Rev. D, 2001, **63**: 074009
23 Bondar A E, Chernyak V L. Phys. Lett. B, 2005, **612**: 215
24 Ball P. J. High Energy Phys., 1998, **09**: 005; Ball P, J. High Energy Phys., 1999, **01**: 010; Ball P, Zwicky R. Phys. Rev. D, 2005, **71**: 014015; Ball P, Braun V M, Lenz A. J. High Energy Phys., 2006, **05**: 004